Special Issue: Thin-films for Sustainable Manufacturing (ICTFPA 2022)

Institution of MECHANICAL ENGINEERS

Journal of ENGINEERING MANUFACTURE

Proc IMechE Part B:
J Engineering Manufacture
1–12

DOI: 10.1177/09544054231157963
journals.sagepub.com/home/pib
SAGE

# Effects of roughing, finishing, and aggressive machining conditions on the milling performance of AISI 1045 steel using TiAlN coated inserts

**S S Rajput[1], C Upadhyay[2], S Gangopadhyay[1] and F Fernandes[3,4]**

**Abstract**

The objective of the present study is to develop a better understanding of machining performance of TiAlN coated tools during face milling of AISI 1045 medium carbon steel. The influences of three different cutting conditions (roughing, finishing, and aggressive conditions) were investigated on cutting forces, chip temperature, tool wear, surface roughness, and chip characteristics. The highest cutting forces were obtained under roughing condition, while, aggressive mode of machining (high values of cutting speed, feed, and depth of cuts) resulted in the highest chip temperature, crater, and flank wear. Material adhesion and coating delamination were predominant under roughing condition. On the other hand, aggressive condition exhibited diffusion wear causing large depth of crater and severe thermal cracks leading to fracture of the cutting edge. Attrition and abrasion wear were also evident. The results of cutting forces, chip temperature, surface roughness, and chip characteristics were correlated with those of tool wear. Results were found to be beneficial in recommending appropriate criteria for choosing different cutting conditions in face milling of AISI 1045 steel using TiAlN coated insert.

**Keywords**

Face milling, cutting conditions, tool wear, cutting force, chip temperature

Date received: 24 August 2022; accepted: 29 January 2023

## Introduction

In order to meet the challenges faced by the machining industries to augment productivity and at the same time fulfill the commitment to follow stricter environmental regulations, it is important to develop advanced machining strategies. In recent times, the machining industries have been striving to implement dry[1] or near-dry machining in an attempt to curtail the usage of environmentally hazardous cutting fluid. With an aim to address the above challenges, a variety of nitride-based hard compound coatings such as TiN, TiAlN, TiCN, CrN, AlCrN etc, were developed for cutting tool applications.[2–7] These coatings improve the hardness, chemical stability, resistance to oxidation, and wear of the tool finally leading to an increase in the tool life and productivity of machining, as well as promoting the prospect of dry or near-dry machining. In the same context, significant research is being caried out in order to augment the tribological properties of hard coatings.[1,8,9] TiAlN coating, in particular, is one of the popular tool coatings because of its high hardness of around 33 GPa under an elevated working temperature of 800°C and resistance to oxidation.[10]

[1]Department of Mechanical Engineering, Indian Institute of Technology Bhilai, Raipur, Chhattisgarh, India
[2]Department of Mechanical Engineering, National Institute of Technology Rourkela, Odisha, India
[3]CEMMPRE - Centre for Mechanical Engineering Materials and Processes, Department of Mechanical Engineering, University of Coimbra, Coimbra, Portugal
[4]ISEP - School of Engineering, Polytechnic of Porto, Porto, Portugal

**Corresponding authors:**
S Gangopadhyay, Department of Mechanical Engineering, Indian Institute of Technology Bhilai, Raipur 492015, Chhattisgarh, India.
Email: soumya@iitbhilai.ac.in; soumya.mech@gmail.com

F Fernandes, ISEP - School of Engineering, Polytechnic of Porto, Rua Dr. António Bernardino de Almeida 431, Porto, 4200-072, Portugal.
Email: fid@isep.ipp.pt

Milling is one of the most versatile machining processes owing to its capability of generating a large variety of surfaces.[11] Although cemented carbide tools have been used in milling operations owing to their high toughness,[12] insufficient wear resistant properties of cement carbide limited their applications. More advanced tool materials like CBN and ceramic tools were also employed particularly during high-speed milling operations.[13,14] However, these cutting tools are expensive and typically not recommended for low-speed operations like rough-mode machining. The development of hard coatings for cemented carbide tools was not only a more cost-effective alternative, but also coated tools provide versatility of cutting conditions to be adopted.[4,11]

Aslan[14] exhibited superior performance of TiAlN coated tools to their TiCN coated counterparts during end milling of hardened X210 Cr12 cold-work tool steel. This was primarily attributed to better high-temperature properties of TiAlN over TiCN coating. Siwawut et al.[15] showed that Ti-based coatings like TiAlSiN and CrTiAlSiN provided better tool life compared to uncoated carbide inserts, in face milling of cast iron with the cutting speed in the range of 140–300 m/min. In line of these results, Liu et al.[16] found that TiAlN coating applied over $Si_3N_4$ tool improved resistance to tool wear during high-speed face milling of gray cast iron. It was observed that the geometry of the cutting tool also had some role on the performance of PVD hard coatings in milling operations. While both TiAlN and TiAlSiN coatings exhibited similar performance during end-milling of W1.2711 tool steel, TiAlSiN outperformed TiAlN for ball-nose milling cutters in terms of average flank wear.[17] However, there is a scarcity in literature concerning the measurement of cutting forces in face milling operations. In a work reported by Çalışkan et al.,[18] it was observed that different Ti-based coatings such as AlTiN/TiN, TiN/TiAlN and multilayer nanocomposite TiAlSiN/TiSiN/TiAlN could not demonstrate improved performance compared to uncoated tool in terms of cutting forces and surface roughness. Coatings were only effective in mitigating tool wear. An et al.[19] exhibited that an increase of cutting speed from 70 to 110 m/min decreased the cutting forces and surface roughness during hard milling of 30Cr3 steel. It was further observed that increasing the depth of cut or the feed rate, resulted in a degradation of the machined surface. Tool failure was primarily influenced by abrasion and adhesion wear, while AlTiN coating suffered from microchipping and delamination. Okada et al.[20] demonstrated that CBN-rich cutting tools were more effective in high-speed hard milling of steel than coated carbide in terms of tool wear, cutting force, and temperature.

It is observed from the published research work that there is hardly any study on the measurement of cutting zone temperature during face milling of steel or ferrous alloys. The wear mechanism of TiAlN coated carbide inserts in face milling of steel is also relatively scarce. Moreover, the effect of machining parameters particularly pertaining to roughing and finishing conditions is yet to be studied in face milling using TiAlN coated inserts. Therefore, the current research work aimed at investigating the role of different machining conditions such as roughing, finishing and aggressive (combination of high values of cutting speed, feed, and depth of cut) conditions on machining characteristics of AISI1045 medium carbon steel during face milling under dry environment. Machining characteristics were evaluated in terms of cutting forces, chip temperatures, tool wear, surface roughness, and chip characteristics. Particular emphasis was provided to explore the underlying tool wear mechanism under various machining conditions.

## Experimental details

### *Workpiece material and cutting tool*

In the present work, machining was performed on AISI 1045 medium carbon steel. The chosen workpiece material is a common grade of steel used for crankshafts, gears, bolts, connecting rods, etc. Some of the important mechanical properties of AISI 1045 steel are listed in Table 1. The workpiece was cut to the size of 125 mm × 50 mm × 50 mm. A commercially available PVD TiAlN coated insert was mounted on the BT-40 taper face-mill tool holder as shown in Figure 1 Details of the cutting tool along with the cutting conditions are provided in Table 1. TiAlN coating was used in the current study because of its wide application in machining of steel.[21]

To examine the thickness of the coating, fractured cross-section of the coated inserts was observed using field-emission scanning electron microscopy (FESEM, Zeiss, Gemini 500). In order to evaluate the performance of the tool inserts in an unbiased and logical manner, a single insert was utilized for each of the experiments.

### *Cutting parameters*

All the machining experiments were conducted on a three-axis Computer Numeric Control (CNC) vertical machining center (AceMicromatic, India, AMS 540V). In order to investigate the effects of cutting parameters on various face milling characteristics of AISI 1045 steel, three different cutting conditions namely roughing, finishing and aggressive conditions were employed. The detailed cutting parameters under these conditions are provided in Table 1. Rough-mode machining involving a combination of low cutting speed and high feed and depth of cut is adopted in the industry when bulk removal of material is the requirement. Finishing operation is preferred when high surface finish is the major objective and it comprises a combination of high cutting speed and low feed and depth of cut. However, none of these conditions would result in high productivity in machining. Therefore, when the major focus is

**Table 1.** Details of cutting tool, workpiece, and machining conditions.

| | Roughing condition | Finishing condition | Aggressive condition |
|---|---|---|---|
| Cutting speed, $V_c$ (m/min) | 75 | 250 | 250 |
| Feed, $f_r$ (mm/min) | 300 | 50 | 300 |
| Feed/tooth (mm/tooth) | 1.0676 | 0.05341 | 0.3205 |
| Axial depth of cut, $a_p$ (mm) | 1 | 0.4 | 1 |
| Radial depth of cut, $a_r$ (mm) | 5 | 5 | 20 |
| Cutting length/pass, $L$ (mm) | 120 | 120 | 120 |
| Single experimental run | 5 passes | 5 passes | 5 passes |
| Environment | Dry run | Dry run | Dry run |
| Direction of cut | Up milling | Up milling | Up milling |
| Tool specification | Face-milling cutter- 85 mm diameter face milling<br>Industrially coated milling inserts<br>(TPAN 1603PPN PA120) | | |
| Workpiece specification | AISI 1045 Steel<br>Tensile strength- 570–700 MPa,<br>Brinell hardness no.- 170–210 | | |

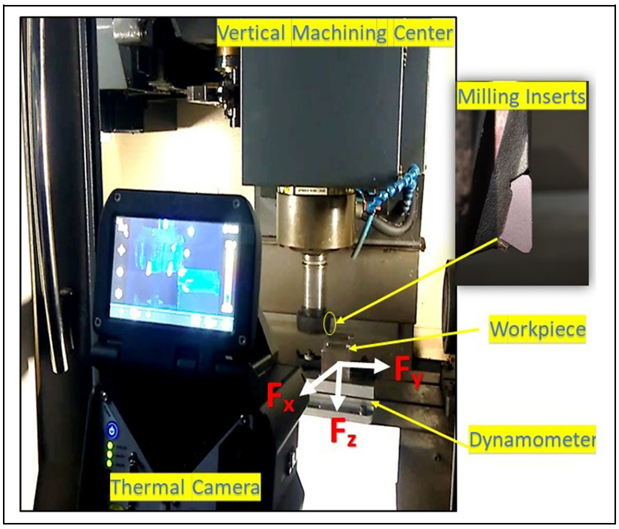


**Figure 1.** Photographic image of the experimental setup.

on achieving high productivity in machining, a combination of high values of all the cutting parameters needs to be adopted. This parametric combination is termed as aggressive condition in the current study since the combination of cutting speed, feed, and depth cut would potentially result in high mechanical and thermal deformation during machining. The selection of cutting parameters under different conditions was based on review of past literatures and a series of pilot experiments. All the experiments were performed under dry environment to assess the feasibility of using TiAlN coated tool for dry machining. Each experimental run was repeated thrice to improve the statical accuracy of measurement of various machining characteristics to be discussed later.

### *Machining characteristics*

Effects of different conditions were studied on a variety of machining characteristics such as cutting forces, chip temperature, tool wear, surface roughness, and chip characteristics during face milling of AISI 1045 under dry environment. Cutting forces were measured using a piezoelectric-type dynamometer (Kistler 9257B) mounted on the machine table as shown in Figure 1. The dynamometer was connected with an eight-channel charge amplifier (5001A) and data acquisition system (DAQ) for acquiring $X$, $Y$, and $Z$ components of cutting forces ($F_x$, $F_y$, and $F_z$ respectively) during machining. Chip temperature was calculated from the cutting temperature field measured by an infrared thermal imaging camera (FLIR X6540sc). The camera was calibrated for the temperature range of 350°C−1200°C. The emissivity of the workpiece was considered as 0.8 after a series of calibration experiments. Similar methodology of measurement of cutting temperature was reported by previous researchers.[22,23]

Each tool insert was disengaged after five machining passes and average flank wear was measured using a stereo-zoom microscope (LEICA S9i). Machining was continued till 25 machining passes for all the cutting conditions so that a comparative evaluation of tool wear and other machining characteristics could be performed. Additionally, the depth of crater formed after 25 passes of face milling was measured using a non-contact type surface profilometer (Sensofar, Model: S neox). Rake and flank surfaces of the inserts after 25 passes of face milling were also investigated using FESEM and Energy-dispersive X-ray spectroscopy (EDS) through X-ray (EDAX,). Microscopic images of the chips were captured using the stereo-zoom microscope after each experimental run. The thickness of the chips at the maximum cross-sectional area was measured using a digital micrometer (Mitutoyo C/N 342-251-30) with a least count of 0.01 mm.

The surface roughness ($R_a$) of the machined workpiece was quantified using a roughness tester (Taylor and Hobson, Surtronic S-100) with cut-off and sampling lengths of 0.8 and 4 mm, respectively. At least five repetitions were performed to improve the statistical accuracy of measurement.

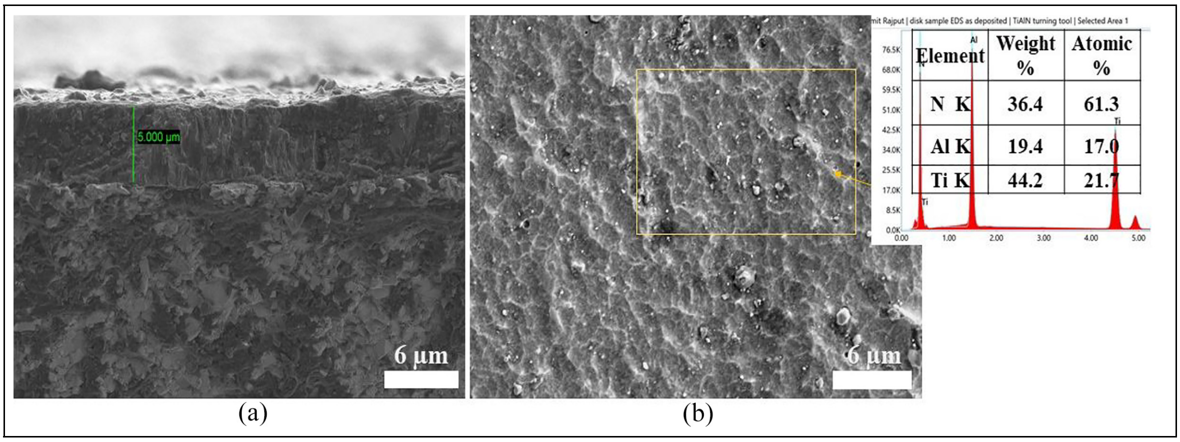


**Figure 2.** (a) Fractograph and (b) surface morphology along with EDS data for commercially available TiAlN coating.

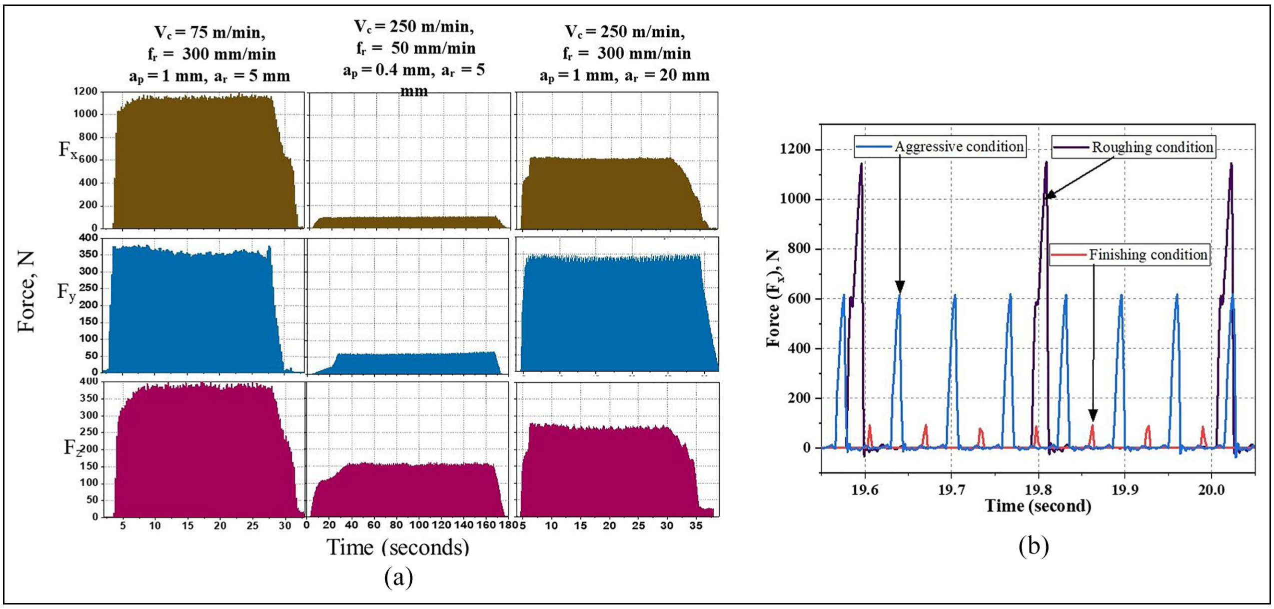


**Figure 3.** Representative profile of cutting forces ($F_x$, $F_y$, and $F_z$) under roughing, finishing, and aggressive conditions for (a) the entire experimental fifth run and (b) shorter duration.

## Results and discussion

Since commercially available TiAlN coating was used in the current study, its background information such as deposition technique and characteristics were not known. Therefore, some basic characterization was needed to reveal the same. Figure 2 shows FESEM images of the coating fractograph and surface morphology of TiAlN coating. A coating thickness of 5 µm could be visible from the image. The coating was dense and compact with hardly any visible defect at the interface indicating the coating possessed strong interfacial strength. The presence of microdroplets on the surface of TiAlN coating indicates cathodic arc deposition might have been utilized to deposit the coating. Several researchers demonstrated similar surface morphology of the coating deposited by cathodic arc evaporation.[24,25] Chemical composition of TiAlN coating is provided in Figure 2(b) using EDS. Since around 44 wt. % of Ti and 20 wt. % of Al are present in TiAlN, relative content of Ti with reference to Al is more than 50%. Higher content of Ti than Al is preferred in TiAlN coating system for superior tribological properties.[21]

Variation of different cutting forces along $X$, $Y$, and $Z$ directions, that is, $F_x$, $F_y$, and $F_z$ in milling operation with time are provided in Figure 3. While force signals for the entire duration of cut are shown in Figure 3(a), a magnified view of the same force signals for shorter duration (~0.5 s) during fifth run is presented in Figure 3(b). Evidently, $F_x$ measured along the direction of table feed showed higher values than $F_y$ and $F_z$. Moreover, maximum forces were obtained under the roughing condition, while minimum forces were

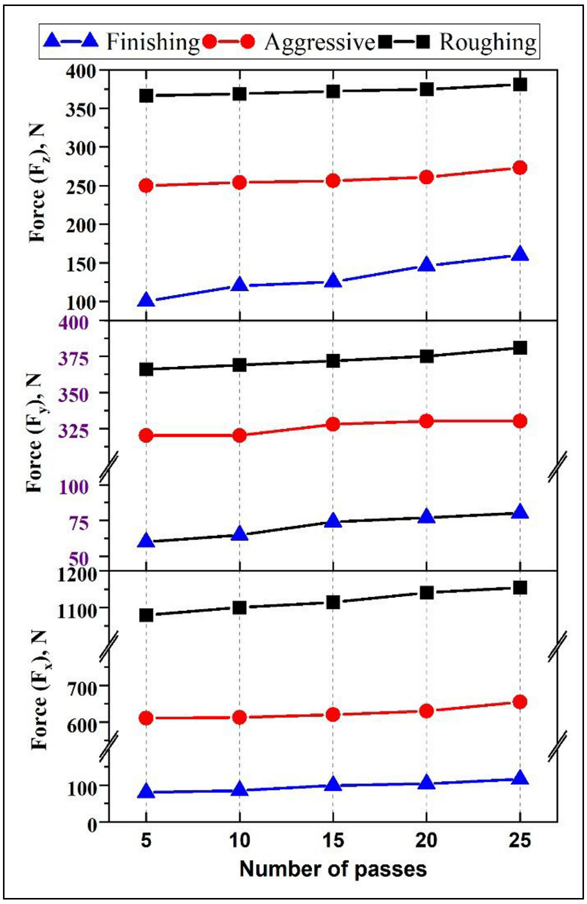


**Figure 4.** Variation of cutting forces ($F_x$, $F_y$, and $F_z$) with number of passes under roughing, finishing, and aggressive conditions.

recorded under finishing condition.[26] This is attributed to the fact that roughing condition has higher feed and depth of cut, as shown in Table 1, than finishing condition. Moreover, higher cutting speed (as in finishing condition) is always associated with lowering the cutting forces due to higher cutting temperature and hence thermal softening of workpiece materials.[27,28] Similarly, as the cutting speed was higher in aggressive condition than the roughing mode, the former resulted in lower forces. At the same time, aggressive condition by virtue of higher feed and depth of cut caused an escalation in forces compared to those under finishing condition. Figure 3(a) also indicates $F_z$ is slightly higher than $F_y$ under roughing and finishing conditions. However, aggressive condition caused a reversal of the situation as $F_y$ was higher than $F_z$. This was due to the higher radial depth of cut in aggressive condition than the other modes of machining. The results also indicate that the influence of radial depth of cut is the highest on $F_y$. Little consideration would also indicate that in Figure 3(b) signals for $F_x$ are symmetric under finishing and aggressive conditions, whereas the signal shows a gradual increase and vertical fall during roughing condition. This may be explained by the lower cutting speed causing slower engagement during the entry.

Variation of different cutting forces with cutting length under different machining conditions is shown in Figure 4. With increasing number of passes, the component of cutting forces exhibits an upward trend. These variations might be attributed to a variety of causes, including tool wear, work hardening of the workpiece material, and cutting temperature. Figure 4 also demonstrates that there is no significant change in the $F_z$ component, indicating that it is the least sensitive to tool wear. During milling, it is essential to evaluate the machining temperature since it can have a detrimental effect on the surface quality and tool life, leading to unstable machining or damage to the tool and workpiece.[29,30]

Figure 5 shows a representative image of the temperature profile of the chips formed during roughing

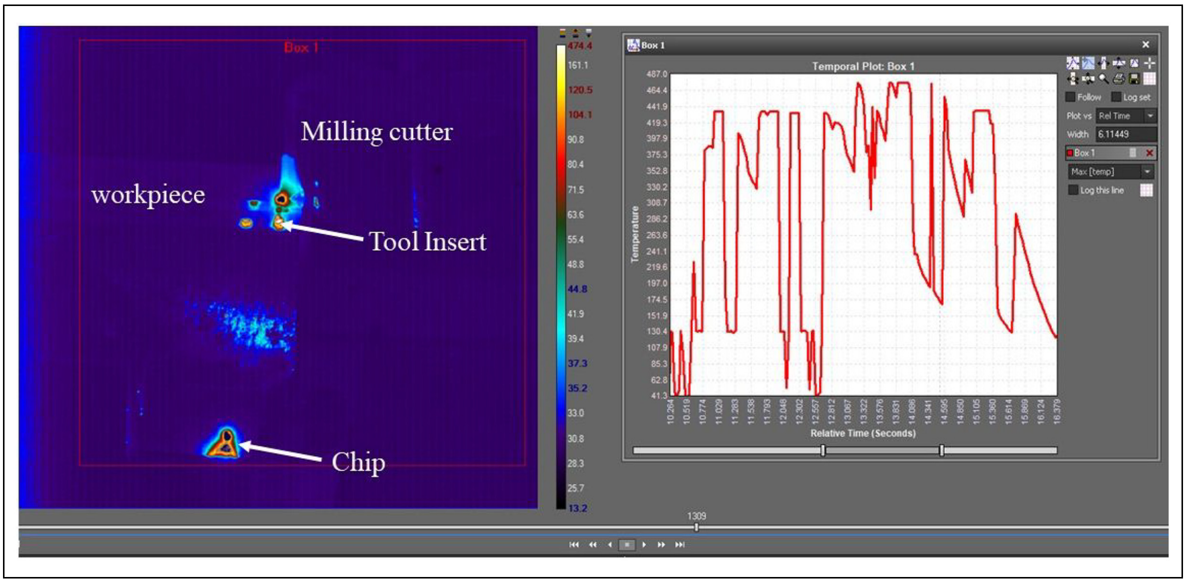


**Figure 5.** Representative temperature profile of chip during machining under roughing condition (during fifth pass).

condition in milling and the variation of maximum temperature with time. Nature of fluctuation of maximum temperature is typical of a milling operation which is an intermittent cutting process.

Figure 6 demonstrates variation of chip temperature with progressive machining runs under different machining conditions. It is evident that rough-mode milling produced the lowest chip temperature, whereas aggressive cutting condition caused the highest chip temperature during cutting. The temperature generated during finishing mode was closer to but less than that in aggressive condition, but much higher (approximately 25%) than in roughing condition. For example, mean values of maximum chip temperature after fifth run were around 445°C, 550°C, and 575°C under roughing, finishing and aggressive conditions respectively. This was due to the fact that milling operation under both roughing and aggressive modes was carried out at high cutting speed of 250 m/min, while the same under roughing mode was 75 m/min as shown in Table 1. Although feed and depth of cut were higher under aggressive condition than finish-mode, the temperature rise was only 25°C. This clearly indicates that cutting speed plays a more dominant role than feed and depth of cut in generating cutting temperature. This argument is in agreement with that reported in previous studies[31,32]

Figure 6 also reveals that chip temperature increased with the number of machining runs which could be attributed to the progressive increase of tool wear. Therefore, the results on chip temperature are in coherence with those of cutting forces presented in Figure 4. Another observation in Figure 6 is the slope of change in chip temperature with the machining runs. Aggressive condition caused steeper increase in temperature as compared to those in roughing and finishing conditions. This observation might be indicative of the fact that tool wear could be more under the aggressive condition which will be discussed later. Higher tool wear with the progression of machining causes the cutting edge to become blunt leading to higher frictional rubbing with the workpiece and hence rise in both force and temperature.[20]

Figure 7 shows SEM image of the rake surface under low magnification along with 2-D surface profile to explore the crater wear. SEM image of the rake surface under rouging and finishing mode did not reveal much damage, but that under aggressive condition depicted clear indirection of crater wear. 2-D surface profile (Figure 7(d)) confirmed significant crater wear took place under aggressive condition. Material adhesion under roughing condition was also evident from Figure 7(d). No significant crater wear or material adhesion could be visible under finishing condition. Lower cutting speed under roughing condition resulted in material adhesion. A combination of higher cutting speed, feed, and depth of cut under aggressive condition caused significant crater wear due to the highest cutting temperature and reasonably high cutting forces

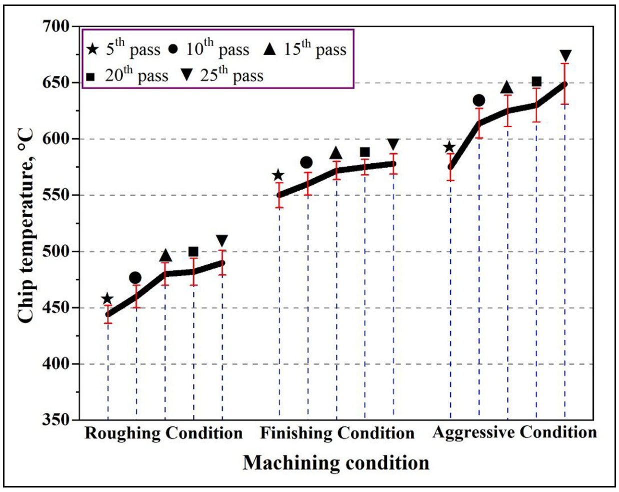


**Figure 6.** Variation of chip temperature with number of passes under roughing, finishing, and aggressive conditions.

as shown in Figures 4 and 6, respectively. Crater wear is primarily caused by diffusion wear.

Magnified SEM image in Figure 8 depicts three different zones such as substrate (Zone-1), adhered material (Zone-2), and combination of adhered material and coating (Zone-3). All the three zones have been depicted in Figure 8(a) and (b) under roughing and finishing condition respectively. However, because of the excessive wear under aggressive condition, zones were not clearly defined (Figure 8(c)). Since the cutting force was the highest under roughing condition, stress at the cutting edge was also maximum causing delamination of coating at Zone-1. Removal of coating is evident from EDS analysis presented in Figure 8(d) with the largest weight % of substrate element (W). Attrition wear was noticeable in Figure 8(a) and (b), particularly in Zone-1. The area in the close proximity of the cutting edge that is, Zone-2, indicates sticking of chip thereby causing material adhesion. This can be observed as excessive amount of Fe in EDS scan of Zone-2 (Figure 8(e)). In Zone-3, that is, beyond Zone-2 both coating and adhered materials were detected from the results of EDS (Figure 8(f)). According to Kuram,[2] coating delamination is the consequence of material adhesion and thermo-mechanical stress. Therefore, coating delamination and significant crater wear took place under aggressive condition owing to diffusion wear at high temperature and greater thermo-mechanical stress under the same condition. Cavitation was visible in Zone-2 under finishing mode possibly due to high cutting temperature.[33] Moreover, thermal cracks were visible under finishing condition. These thermal cracks were formed due to cyclic fluctuation of chip temperature which is a characteristic feature of the milling operation. Naturally, the effects were more pronounced with the rise in machining zone temperature. Therefore, it is evident from Figure 8(c) that thermal crack grew more severe resulting in fracture of the cutting edge under aggressive condition.[29,30]

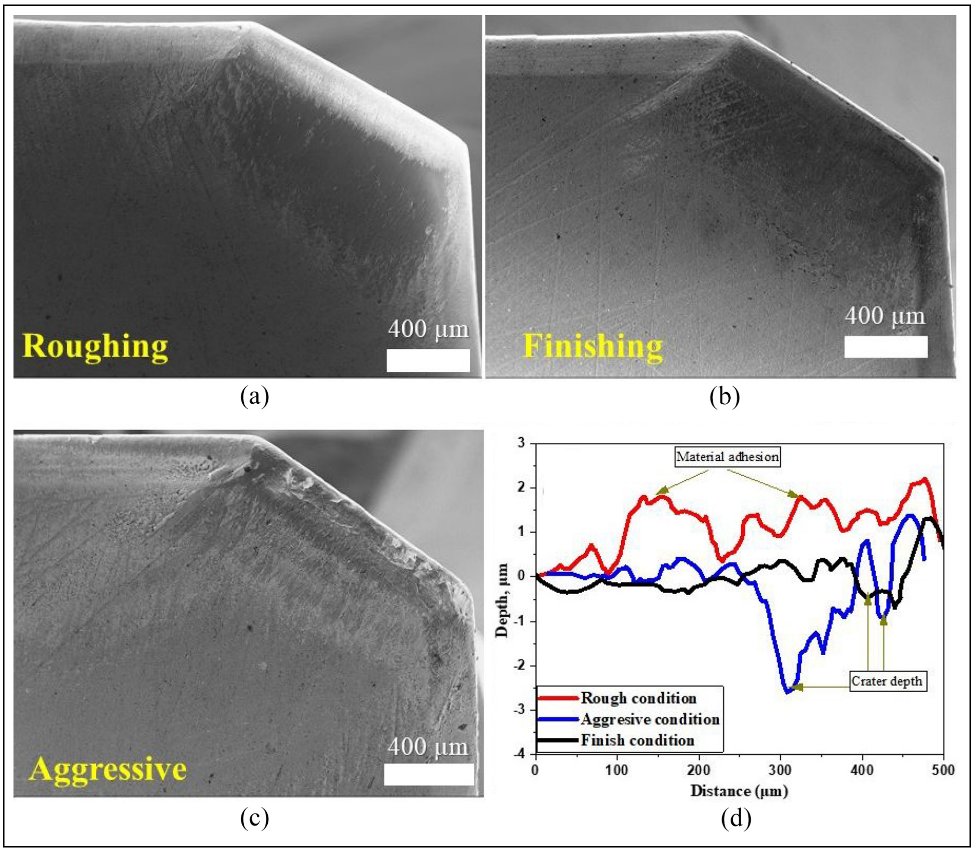


**Figure 7.** SEM images of rake surface of TiAlN coated tool under (a) roughing, (b) finishing, (c) aggressive conditions, and (d) 2D surface profile of the rake surface.

Figure 9 presents the SEM images of the flank surface under all the three conditions, as well as the corresponding EDS elemental maps. Evidently, flank wear was the highest under aggressive condition owing to the greater degree of abrasion caused due to combination of higher values of cutting parameters. Careful observation of elemental maps in Figure 9(b) indicates different zones. Just beneath the cutting edge, evidence of material adhesion comprising of oxides of iron was detected. Evidence of oxidation was more pronounced under finishing and aggressive condition with high value of cutting speed (250 m/min). This result indicates that oxidation wear is one of the wear mechanisms particularly under high-speed condition.[34] This zone was followed by the presence of coating and finally a combination of adhered material and coating. Similar observation was also reported by Sousa et al.[17]

Figure 10 demonstrates the progression of average flank wear with the number of machining passes under all the three conditions. It is evident that the rate of increase in flank wear was the highest under the aggressive condition. Therefore, the results of flank wear directly corroborate the ones pertaining to the slope of increase in chip temperature presented in Figure 6. Moreover, average flank wear under roughing condition was slightly higher (approximately 17%) than that in finishing mode. This might be explained by the fact that cutting forces were much higher under roughing than in finishing condition although cutting temperature was less in roughing mode. Therefore, it may be concluded that cutting force has slightly greater influence over cutting temperature on average flank wear in milling operation. It is also noteworthy to mention that the coated tool did not reach wear threshold of 0.3 mm (as per ISO 8688-2) even after 25 numbers of passes under aggressive condition owing to excellent wear resistant properties of TiAlN coating.

Figure 11 shows variation of surface roughness ($R_a$) of machined workpiece with the number of machining passes under all the three conditions. It is evident from the figure that roughing condition resulted in maximum surface roughness which was ascribed to high feed (1.067 mm/tooth) and low cutting speed (75 m/min). Although finishing condition exhibited the lowest surface roughness, it was significantly higher than theoretically expected value of $R_a$, since there was 20 times reduction in feed (0.053 mm/tooth) coupled with rise in cutting speed (250 m/min) of more than three times. Such increase in roughness was possibly connected to various phenomena like cutting temperature, tool wear, migration of foreign particles on the finished surface etc. Although those phenomena were not significant in a broader sense, they were still enough to increase the $R_a$ value by around 0.1 μm or less with reference to the

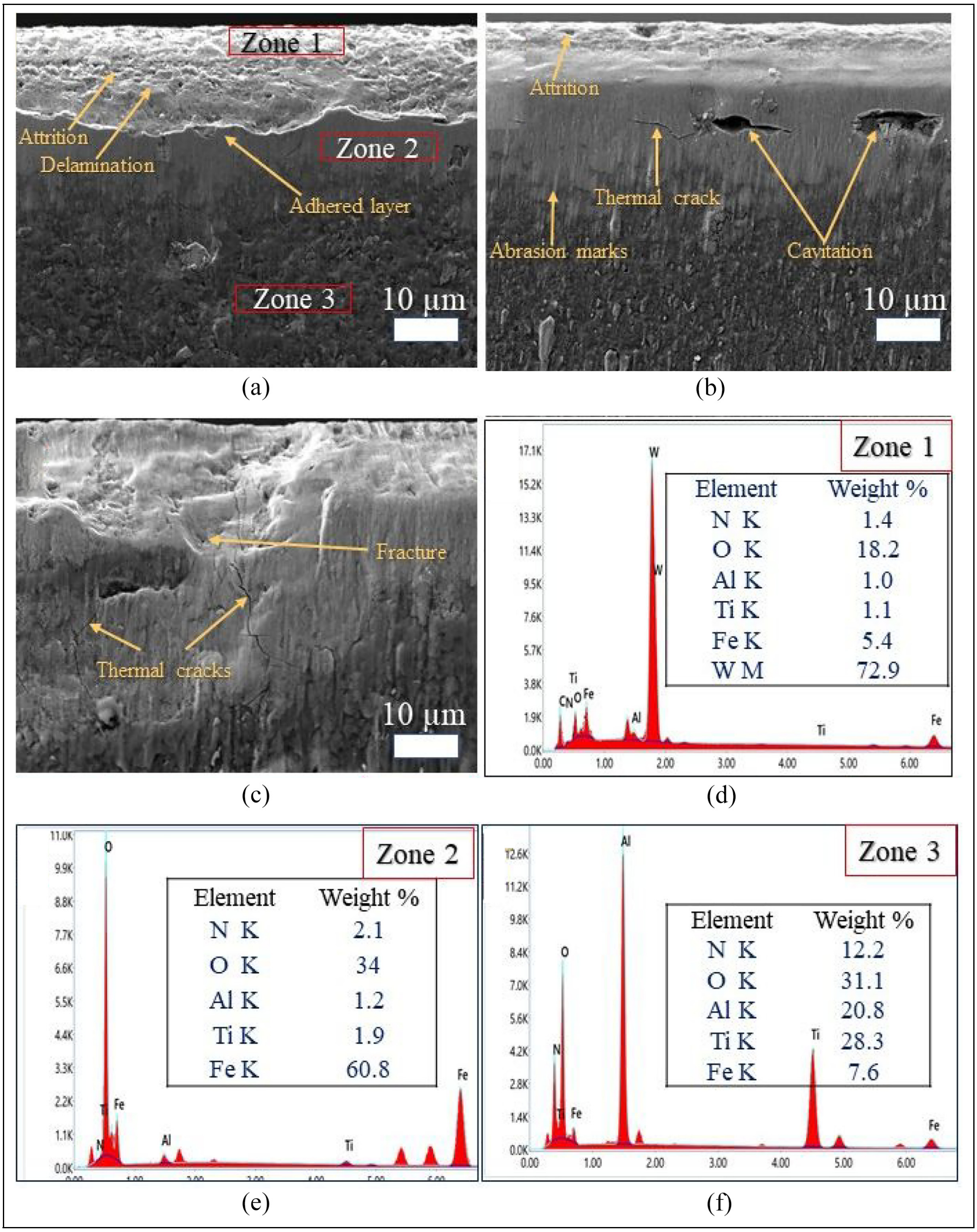


**Figure 8.** Magnified SEM images of rake surface near cutting edge under (a) roughing, (b) finishing, (c) aggressive conditions and EDS results at (d) zone-1, (e) zone-2, and (f) zone-3.

theoretically expected value. With reference to the roughing condition, there was more than three times increase in cutting speed and three times decrease in feed under aggressive condition. As a combined effect, there was a reduction of surface roughness by around 88% which was more or less in the range of expected value of surface roughness. When surface roughness between finishing and aggressive conditions was compared, the difference was not very significant although there was ~6 times increase in feed under aggressive condition compared to that under finishing condition. Due to the same reason as explained above, the experimental value of $R_a$ under finishing condition was higher than the theoretically expected value.

Similar to cutting forces and temperature, influence of tool wear on surface roughness was evident with the

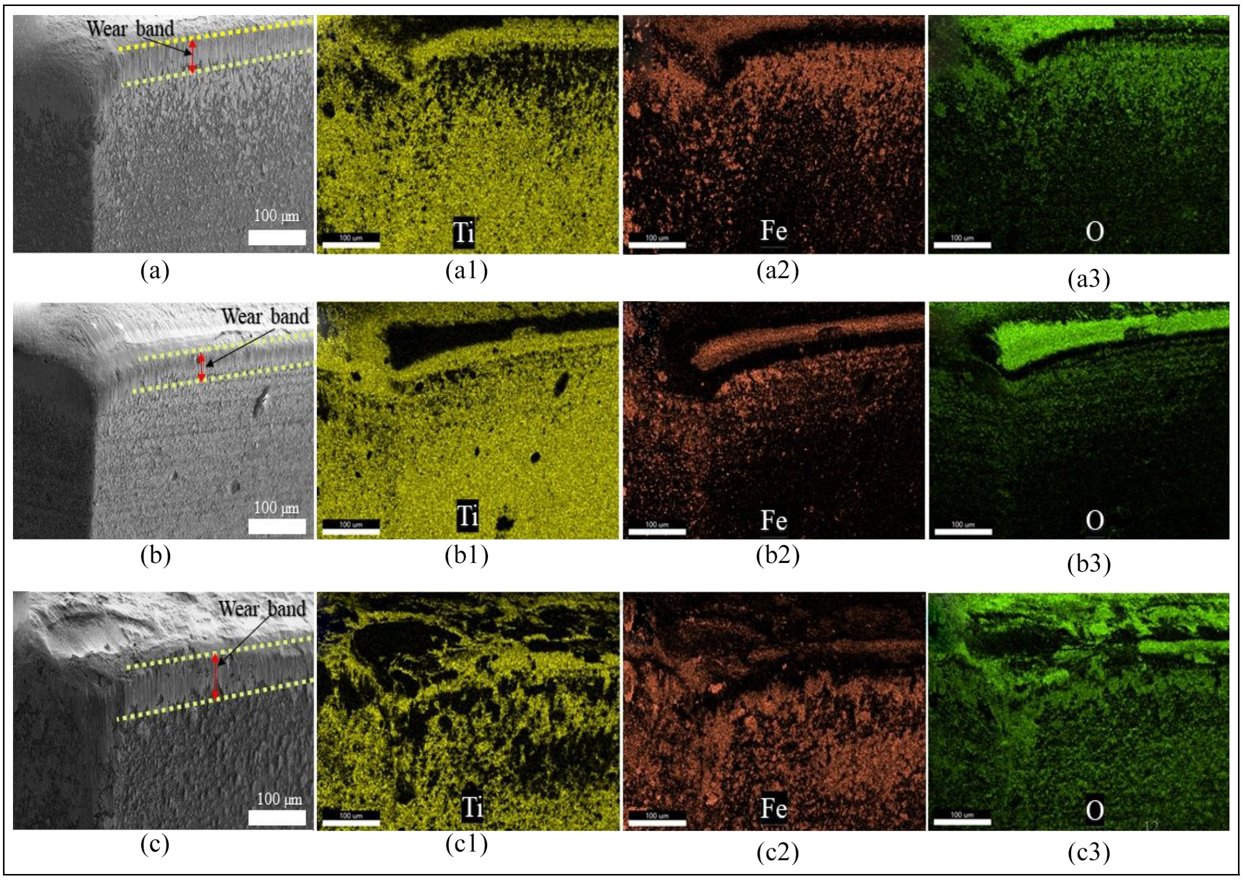


**Figure 9.** SEM images of flank surfaces under (a) roughing, (b) finishing, and (c) aggressive conditions with the corresponding elemental mapping at the same regions.

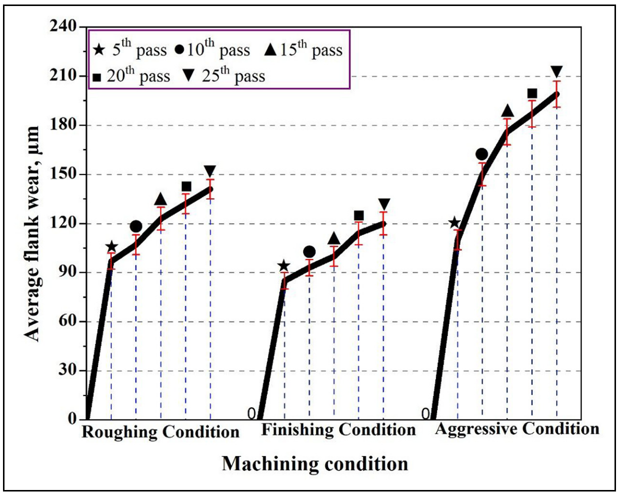


**Figure 10.** Progression of average flank wear with the number of passes under different conditions of machining.

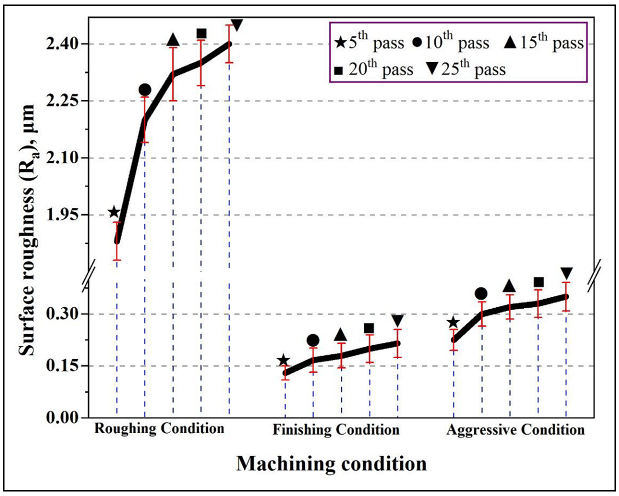


**Figure 11.** Variation of surface roughness with number of passes under different conditions of machining.

gradual increase in $R_a$ value with the number of machining passes as shown in Figure 11.

Chip thickness obtained under all the three conditions, shown in Figure 12, demonstrated the lowest value (84% lesser than aggressive condition) under finishing mode and the highest value (82% higher than aggressive condition) under roughing mode. This observation was in coherence with that of cutting forces. Since cutting forces were higher under roughing condition, the degree of deformation was maximum and so was chip thickness. The trend of cutting forces and hence deformation under finishing and aggressive

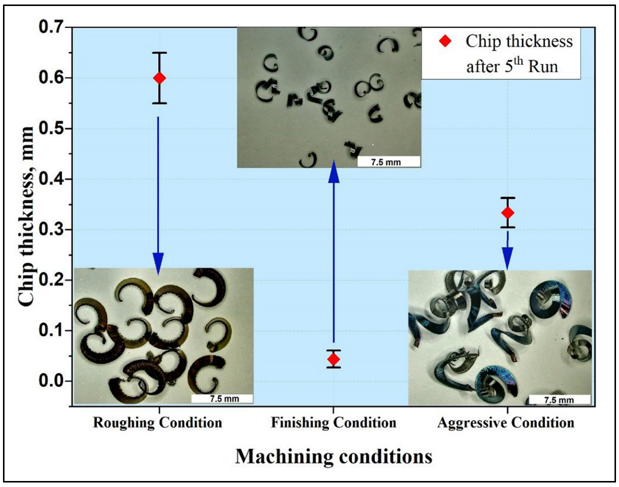


**Figure 12.** Chip thickness and microscopic images of the chips under different conditions of machining.

conditions similarly influenced the chip thickness under the same conditions. Chips under roughing and finishing conditions showed C-type morphology as evident from Figure 12. Aggressive conditions exhibited similar chip morphology but with a slightly larger length of the chip. This is attributed to higher radial depth of cut under aggressive condition than the other ones. Moreover, chips under aggressive condition had bluish appearance, while the other chips did not undergo noticeable change in color. This can be explained by the fact that the chips were subjected to significant oxidation due to highest temperature under the aggressive condition (Figure 6).

The results from the present work could be helpful in choosing appropriate cutting condition while using TiAlN coated tool insert in face milling operation depending on the requirement. Aggressive condition should be given preference if the objective is stock removal of material while maintaining reasonable surface finish without much regard to tool wear. Roughing condition should be adopted when surface finish is not a major issue, but material removal from the workpiece while maintaining low tool wear rate is in the focus. For superior surface finish along with low tool wear rate, finishing condition should always be chosen.

## Conclusions

In this research work, face milling of AISI 1045 steel was studied using TiAlN coated inserts under roughing, finishing, and aggressive conditions of machining. Based on the results the following conclusions could be derived.

- Roughing condition exhibited maximum cutting force followed by aggressive and finishing conditions. High feed and depth of cut coupled with low cutting speed resulted in higher frictional drag and material adhesion causing escalation of cutting forces.
- Owing to low cutting speed, roughing condition resulted in the lowest chip temperature, while maximum temperature was recorded under aggressive condition.
- Roughing condition exhibited coating delamination, attrition and adhesion wear due to lower cutting speed. Thermal cracks were less severe under finishing mode, while aggressive condition promoted more severe thermal cracks leading to fracture of cutting edge. The highest depth of crater was also obtained under the same condition due to diffusion wear. Oxidation wear was also prominent under the condition of high cutting speed.
- Average flank wear was maximum under aggressive condition due to combination of high cutting parameters. Flank wear was slightly higher under roughing than the finishing condition. By virtue of excellent wear resistance properties of TiAlN coating, the tool did not reach the wear threshold of 0.3 mm even after 25 number of passes.
- High surface roughness and chip thickness under rouging condition were attributed to low cutting speed and higher cutting force.

Results from the current study were found be beneficial in recommending the criteria of choosing aggressive, roughing and finishing conditions with reference cutting forces, tool wear, surface roughness, and material removal from the detailed analysis of the results.


### Declaration of conflicting interests

The author(s) declared no potential conflicts of interest with respect to the research, authorship, and/or publication of this article.

### Funding

The author(s) disclosed receipt of the following financial support for the research, authorship, and/or publication of this article: S Gangopadhyay would like to thank the Department of Science and Technology, Government of India for funding the research work under the bilateral collaborative project between India and Portugal (Project No. DST/INT/Portugal/P-14/2017). This research is also sponsored by FEDER Funds through Portugal 2020 (PT2020), by the Competitiveness and Internationalization Operational Program (COMPETE 2020) and national founds through the Portuguese Foundation for Science and Technology (FCT), under the projects: SMARTLUB – ref. "POCI-01-0145-FEDER-031807" MCTool21- ref:" POCI-01-0247-FEDER-045940″ and CEMMPRE -ref. "UIDB/00285/2020" Bilateral collaborative project between Portugal and India (Project number 441.00 INDIA) is also acknowledged.

## ORCID iDs

C. Upadhyay https://orcid.org/0000-0003-2465-9486
S. Gangopadhyay https://orcid.org/0000-0002-0986-8362
F. Fernandes https://orcid.org/0000-0003-4035-3241

## References

1. Fernandes F, Danek M, Polcar T, et al. Tribological and cutting performance of TiAlCrN films with different Cr contents deposited with multilayered structure. *Tribol Int* 2018; 119: 345–353.
2. Kuram E. The effect of monolayer TiCN-, AlTiN-, TiAlN-and two layers TiCN + tin- and AlTiN + TiN-coated cutting tools on tool wear, cutting force, surface roughness and chip morphology during high-speed milling of Ti6Al4V titanium alloy. *Proc IMechE, Part B: J Engineering Manufacture* 2018; 232: 1273–1286.
3. Durmaz YM and Yildiz F. The wear performance of carbide tools coated with TiAlSiN, AlCrN and TiAlN ceramic films in intelligent machining process. *Ceram Int* 2019; 45: 3839–3848.
4. Sampath Kumar T, Ramanujam R, Vignesh M, et al. Comparative evaluation of performances of TiAlN, AlCrN, TiAlN/AlCrN coated carbide cutting tools and uncoated carbide cutting tools on turning Inconel 825 alloy using grey relational analysis. *Sens Actuators A Phys* 2018; 279: 331–342.
5. Thakur A and Gangopadhyay S. Evaluation of micro-features of chips of Inconel 825 during dry turning with uncoated and chemical vapour deposition multilayer coated tools. *Proc IMechE, Part B: J Engineering Manufacture* 2018; 232: 979–994.
6. Dumkum C, Jaritngam P and Tangwarodomnukun V. Surface characteristics and machining performance of TiAlN-, TiN- and AlCrN-coated tungsten carbide drills. *Proc IMechE, Part B: J Engineering Manufacture* 2019; 233: 1075–1086.
7. Mativenga PT and Hon KKB. A study of cutting forces and surface finish in high-speed machining of AISI H13 tool steel using carbide tools with TiAlN based coatings. *Proc IMechE, Part B: J Engineering Manufacture* 2003; 217: 143–151.
8. Rajput SS, Gangopadhyay S, Yaqub TB, et al. Room and high temperature tribological performance of CrAlN(Ag) coatings: the influence of Ag additions. *Surf Coat Technol* 2022; 450: 129011.
9. Ju H, Zhou R, Luan J, et al. Tribological performance under different environments of Ti – C – N composite films for marine wear-resistant parts. *Int J Miner Metall Mater* 2022; 30: 144–155.
10. Xu YX, Chen L, Pei F, et al. Thermal stability and oxidation resistance of V-alloyed TiAlN coatings. *Ceram Int* 2018; 44: 1705–1710.
11. Sousa VFC and Silva FJG. Recent advances on coated milling tool technology—A comprehensive review. *Coatings* 2020; 10: 235.
12. Song X, Gao Y, Liu X, et al. Effect of interfacial characteristics on toughness of nanocrystalline cemented carbides. *Acta Mater* 2013; 61: 2154–2162.
13. Becze CE, Clayton P, Chen L, et al. High-speed five-axis milling of hardened tool steel. *Int J Mach Tools Manuf* 2000; 40: 869–885.
14. Aslan E. Experimental investigation of cutting tool performance in high speed cutting of hardened X210 Cr12 cold-work tool steel (62 HRC). *Mater Des* 2005; 26: 21–27.
15. Siwawut S, Saikaew C, Wisitsoraat A, et al. Cutting performances and wear characteristics of WC inserts coated with TiAlSiN and CrTiAlSiN by filtered cathodic arc in dry face milling of cast iron. *Int J Adv Manuf Technol* 2018; 97: 3883–3892.
16. Liu W, Chu Q, Zeng J, et al. PVD-craln and TiAlN coated Si3N4 ceramic cutting inserts-2. High speed face milling performance and wear mechanism study. *Ceram Int* 2017; 43: 9488–9492.
17. Sousa VFC, Silva FJG, Alexandre R, et al. Study of the wear behaviour of TiAlSiN and TiAlN PVD coated tools on milling operations of pre-hardened tool steel. *Wear* 2021; 476: 203695.
18. Çalışkan H, Kurbanoğlu C, Panjan P, et al. Investigation of the performance of carbide cutting tools with hard coatings in hard milling based on the response surface methodology. *Int J Adv Manuf Technol* 2013; 66: 883–893.
19. An Q, Wang C, Xu J, et al. Experimental investigation on hard milling of high strength steel using PVD-AlTiN coated cemented carbide tool. *Int J Refract Metals Hard Mater* 2014; 43: 94–101.
20. Okada M, Hosokawa A, Tanaka R, et al. Cutting performance of PVD-coated carbide and CBN tools in hard-milling. *Int J Mach Tools Manuf* 2011; 51: 127–132.
21. Aihua L, Jianxin D, Haibing C, et al. Friction and wear properties of TiN, TiAlN, AlTiN and CrAlN PVD nitride coatings. *Int J Refract Metals Hard Mater* 2012; 31: 82–88.
22. Liu C, He Y, Wang Y, et al. Effects of process parameters on cutting temperature in dry machining of ball screw. *ISA Trans* 2020; 101: 493–502.
23. Zhang H, Dang J, Ming W, et al. Cutting responses of additive manufactured Ti6Al4V with solid ceramic tool under dry high-speed milling processes. *Ceram Int* 2020; 46: 14536–14547.
24. Kulkarni AP, Joshi GG and Sargade VG. Performance of PVD AlTiCrN coating during machining of austenitic stainless steel. *Surf Eng* 2013; 29: 402–407.
25. Zhang K, Deng J, Ding Z, et al. Improving dry machining performance of TiAlN hard-coated tools through combined technology of femtosecond laser-textures and WS2 soft-coatings. *J Manuf Process* 2017; 30: 492–501.
26. Hosseini E, Rehman S and Alimoradi A. Optimization of turn-milling process in roughing and finishing regimes: trade-off between productivity, cutting force and surface integrity. *Proc IMechE, Part E: J Process Mechanical Engineering* 2021; 235: 1383–1395.
27. Cui X, Guo J, Zhao J, et al. Chip temperature and its effects on chip morphology, cutting forces, and surface roughness in high-speed face milling of hardened steel. *Int J Adv Manuf Technol* 2015; 77: 2209–2219.
28. Shi K, Zhang D, Ren J, et al. Effect of cutting parameters on machinability characteristics in milling of magnesium alloy with carbide tool. *Adv Mech Eng* 2016; 8: 1–9.
29. Liu ZQ, Ai X, Zhang H, et al. Wear patterns and mechanisms of cutting tools in high-speed face milling. *J Mater Process Technol* 2002; 129: 222–226.
30. Hou J, Zhou W, Duan H, et al. Influence of cutting speed on cutting force, flank temperature, and tool wear in end

milling of Ti-6Al-4V alloy. *Int J Adv Manuf Technol* 2014; 70: 1835–1845.
31. Kikuchi M. The use of cutting temperature to evaluate the machinability of titanium alloys. *Acta Biomater* 2009; 5: 770–775.
32. Zheng G, Xu R, Cheng X, et al. Effect of cutting parameters on wear behavior of coated tool and surface roughness in high-speed turning of 300M. *Measurement* 2018; 125: 99–108.
33. Halim NHA, Haron CHC, Ghani JA, et al. Tool wear and chip morphology in high-speed milling of hardened Inconel 718 under dry and cryogenic CO2 conditions. *Wear* 2019; 426–427: 1683–1690.
34. Cui X, Zhao J and Tian X. Tool wear in high-speed face milling of AISI H13 steel. *Proc IMechE, Part B: J Engineering Manufacture* 2012; 226: 1684–1693.